Title: *Wolbachia* endosymbionts manipulate GSC self-renewal and differentiation to enhance host fertility

Authors: Shelbi L Russell[1]*, Jennie Ruelas Castillo[2], William T Sullivan[3]

Affiliations:

1. Department of Biomolecular Engineering, University of California Santa Cruz, Santa Cruz, CA, United States
2. Division of Infectious Diseases, Department of Medicine, The Johns Hopkins Hospital, Baltimore, MD, United States
3. Department of Molecular, Cell, and Developmental Biology, University of California Santa Cruz, Santa Cruz, CA, United States

*** corresponding author email: shelbilrussell@gmail.com**

Graphical Abstract:

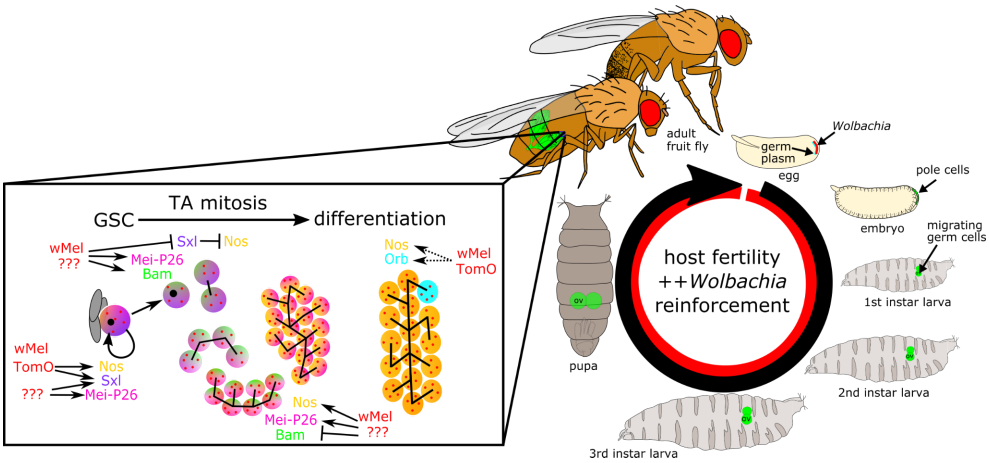

Highlights:

- The wMel strain of *Wolbachia* restores fertility in females and males deficient for the essential translational regulator *meiotic-P26*
- *Mei-P26's* germline maintenance and oocyte cyst differentiation functions are genetically rescued by wMel infection
- Perturbed pMad, Sxl, Bam, and Orb expression are mitigated by wMel infection
- wMel infection elevates lifetime egg lay and hatch rates in wild-type flies

Abstract:

The alphaproteobacterium *Wolbachia pipientis* infects thousands of arthropod and nematode species worldwide, making it a key target for host biological control. *Wolbachia*-driven host reproductive manipulations, such as cytoplasmic incompatibility (CI), are often credited for catapulting these intracellular bacteria to high frequencies in their host populations. Positive, perhaps mutualistic, reproductive manipulations may also increase infection frequencies, but they are not well understood on molecular, cellular, or organismal levels. Previous studies demonstrated that *Wolbachia* is capable of partially rescuing *sex-lethal*, a gene required for germline stem cell (GSC) self renewal and *bag-of-marbles*, a gene required for GSC differentiation. Here, we identify molecular and cellular mechanisms by which *Wolbachia* is able to influence molecularly distinct processes of GSC self renewal and differentiation through our discovery that the wMel strain rescues *meiotic-P26* mutants. Mei-P26 is an essential translational regulator and is required for both GSC self-renewal and differentiation. We demonstrate that wMel rescues the fertility of flies lacking adequate *mei-P26* dosage and function, and is sufficient to sustain infertile homozygous *mei-P26* hypomorphic stocks indefinitely. Cytology revealed that wMel infection mitigates the impact of *mei-P26* loss on both germline stem cell maintenance and cyst differentiation through restoring proper pMad, Bam, Sxl, and Orb expression. Rescue in males, amplification of dominant negative effects, and multiallelic rescue suggest that wMel either directly or indirectly replaces Mei-P26 function. Even in wild-type individuals, wMel infection elevates lifetime egg lay and hatch rates. Over time, the beneficial fertility reinforcement mechanisms described here may promote the emergence of mutualism and the breakdown of CI.

Introduction:

Endosymbiotic bacteria have evolved diverse strategies for infecting and manipulating host populations (*1*, *2*), which are now being leveraged for biological control applications (*3*). Many of these bacteria reside within host cells and navigate female host development to colonize offspring, thus linking their fitness to that of their hosts through vertical transmission (*4*). Endosymbionts with reproductive manipulator capabilities go a step further by altering host development in ways that rapidly increase the frequency of infected, reproductive females in the host population. Reproductive manipulator strategies generally include cytoplasmic incompatibility (CI), where infected sperm require rescue by infected eggs, male-killing, feminization, and parthenogenesis (*5*, *6*). These reproductive manipulations can be highly effective at driving bacterial symbionts into host populations, regardless of costs to the host individual or population (*7*).

Despite the success of parasitic reproductive manipulation, natural selection favors symbionts that increase the fertility of infected mothers, even if these variants reduce the efficacy of the parasitic mechanisms that initially drove the infection to high frequency (*8*). In associations between arthropods and strains of the alphaproteobacterium *Wolbachia pipinensis,* this scenario may be common. For example, measured fecundity in populations of *Drosophila simulans* infected with the wRi strain of *Wolbachia* swung from -20% to +10% across a 20-year span following wRi's CI-mediated sweep across California in the 1980s (*9*). This transition from fitness cost to benefit coincided with weakening of CI strength over the same time-frame (*10*). Fertility-enhancing mechanisms may be at work in other strains of *Wolbachia* that have reached high infection frequencies in their native hosts, yet do not currently exhibit evidence of parasitic reproductive manipulation (*11*). Importantly, these fitness benefits may have also played a role in the early stages of population infection, when infected hosts are at too low of frequencies for CI to be effective (*12*).

Currently, the wMel strain and its encoded CI mechanism are successfully being used to biologically control non-native hosts (*3*). In *Aedes aegypti* mosquitoes, CI causes nearly 100% mortality of offspring born to uninfected mothers (*13*). However, in its native host, the fruit fly *Drosophila melanogaster*, wMel exhibits CI that rarely exceeds 50% mortality and is extremely sensitive to paternal age (*14–16*), as well as grandmother age/female titer (*17*, *18*). Despite weak CI in its native host, wMel is found at moderate to high infection frequencies in populations worldwide (*19*, *20*). Other data suggest that these frequencies may be explained by some emergent beneficial function that increases host fitness (*21–24*). Given that wMel's use in non-native hosts relies on strong and efficient CI, it is essential that we learn the basis for its beneficial functions that could ultimately undermine CI function.

Host germline stem cell (GSC) maintenance and differentiation pathways are powerful targets for *Wolbachia*-mediated reproductive manipulation. *Wolbachia* strains have strong affinities for host germline tissues (*25*, *26*), positioning them at the right place to manipulate and enhance host fertility. In the strains that form obligate associations with *Brugia* filarial nematodes (*27*) and *Asobara* wasps (*28*), *Wolbachia* is required in the germline to prevent premature differentiation and achieve successful oogenesis (reviewed in (*29*)). In the facultative wMel-*D. melanogaster* association, the wMel strain can partially rescue select loss of function alleles of the essential germline maintenance genes *sex-lethal (sxl)* and *bag-of-marbles (bam)* in female flies (*30–32*). It is known that wMel encodes its own factor, Toxic manipulator of oogenesis (TomO), that partially recapitulates Sxl function in the GSC through derepression and overexpression of the translational repressor Nanos (Nos) (*33*, *34*). However, Nos expression is negatively correlated with Bam expression in the early germarium (*35*). Therefore, Bam's function in cyst patterning and differentiation in wMel-infected mutant flies cannot be explained by shared mechanisms with *sxl* rescue or TomO's known functions.

Here, we report that *D. melanogaster* flies infected with the wMel strain of *Wolbachia* are resilient to mutations in the essential fertility gene, *meiotic-P26,* and exhibit enhanced fertility relative to uninfected wild-type flies.

Host *mei-P26* encodes a Trim-NHL protein required for female GSC maintenance (*36*), differentiation (*37*, *38*), and meiosis (*38*, *39*). *mei-P26* confers this range of functions by acting as an adapter for multiple translational repressor complexes through its protein-binding NHL and E3-ligase domains (*36*) (see Figure S1). Infection with wMel is sufficient to maintain GSC maintenance and rescue cyst differentiation indefinitely, in both males and females. Infection mitigates downstream effects of perturbed *mei-P26* function on phosphorylated Mothers against decapentaplegic (pMad), Sxl, Bam, and Oo18 RNA-binding (Orb) protein expression. Next, we find evidence of wMel's beneficial reproductive manipulator abilities in wild-type flies, demonstrating how these phenotypes may be selected for in nature. These results are essential to understanding how wMel reaches high frequencies in natural *D. melanogaster* populations and may be able to be harnessed for biological control applications.

Results

Infection with wMel rescues female D. melanogaster fertility in mei-P26 deficient flies

Flies lacking Mei-P26 function laid significantly fewer eggs and fewer of these eggs hatched into viable offspring than wild-type flies, and wMel infection partially rescued these defects (Figures 1A-C, S2; p=2.2e-16 to 2.9e-2, Wilcoxon Rank Sum; see Tables S1-3). wMel mediated a significant degree of rescue for all allelic strengths and nos:GAL4/UAS-driven RNAi knockdowns, suggesting a robust bacterial rescue mechanism that compensates for loss of protein dosage and function. Rescue was complete for *nos*-driven *mei-P26* RNAi depletion (from 26% deficient offspring production in uninfected flies). Offspring production decreased 94% and 73% in uninfected and wMel-infected *mei-P26[1]* hypomorphic females, respectively, compared to wild-type of the matching infection status. Offspring production decreased 99% and 82% in uninfected and wMel-infected *mei-P26[1]/mei-P26[mfs1]* trans-heterozygous females, respectively. Offspring production decreased 100% and 97% in uninfected and wMel-infected *mei-P26[mfs1]* null females, respectively. Breaking offspring production down into egg lay and egg hatch components revealed that as allelic strength increased, from *nos*-driven RNAi to hypomorphic and null alleles, fertility impacts shifted from those that impacted differentiation/development (egg hatch) to those that also impacted egg production (egg lay).

Infection of *mei-P26* RNAi knockdown females with wMel rescued differentiation defects caused by *mei-P26* loss and elevated fertility relative to wild-type (Figure 1A-E and Table S1-3). Offspring production decreased 26% to 0% in uninfected and wMel-infected nos>mei-P26 RNAi-depleted females, respectively. Instead, wMel-infected *mei-P26* RNAi females produced 44% more offspring than infected wild-type females of the Oregon R (OreR) strain. Offspring production requires successful maintenance of the GSC, differentiation of a GSC daughter cell into a fully developed and fertilized egg, embryogenesis, and hatching into a first-instar larva. Breaking offspring into its egg lay and egg hatch components revealed that nos>RNAi knockdown had a greater impact on the *mei-P26* functions that lead to egg hatch than those that lead to egg production. Egg hatch rate decreased 40% and 16% in uninfected and wMel-infected nos>mei-P26 RNAi-depleted flies, respectively, compared to wild-type of the matching infection status. Uninfected and wMel-infected *nos>mei-P26* RNAi-depleted females exhibited 40% and 16% decrease in egg hatch rate compared to uninfected and wMel-infected wild-type flies, respectively. In contrast, uninfected *mei-P26* RNAi females laid similar numbers of eggs per day as uninfected and infected wild-type (~28 eggs/day). wMel-infected *mei-P26* RNAi females laid 67% more eggs than wild-type, suggesting a synergistic role between wMel and low dose-Mei-P26, potentially through influencing GSC maintenance and/or division.

wMel-mediated *mei-P26* rescue is robust and sufficient to rescue this gene in a stable stock. Infection with wMel elevates both the number of eggs laid and the proportion of those eggs that hatch to produce viable larvae across the fly lifespan in *mei-P26[1]* hypomorphic and *nos*-driven RNAi-knockdown females (p=1.5e-11

to 3.4e-2, Kolmogorov-Smirnov Test; Figure 1F,G, S2A-C). The wMel rescue mechanism is not specific to females, as the impacts of *mei-P26* loss on male fertility are mitigated by wMel-infection (Figure S2D-F; p=6.1e-6 to 2.9e-2, Wilcoxon Rank Sum; see Table S4). Thus, we were able to establish a homozygous stock of *mei-P26[1]* flies infected with wMel *Wolbachia.* In contrast, the uninfected stock only lasted a few weeks (Figure S2G,H) without balancer chromosomes. Given the severe, yet significantly rescuable nature of the *mei-P26[1]* allele, we proceeded with this genotype for many of our subsequent assays for specific immunocytological rescue phenotypes.

Female germline morphology is rescued by wMel infection in mei-P26 deficient flies

Comparing the cytology of *mei-P26* knockdown oocytes infected and uninfected with *Wolbachia* confirmed that wMel-infected ovarioles exhibit far fewer developmental defects than uninfected, more closely resembling wild-type (Figure 1H-K; Vasa (Vas) = germline (*40*), Hu Li Tai Shao (Hts) = cytoskeletal spectrosome/fusome (*41*), propidium iodide (PI)=DNA). Specifically, wMel infected ovarioles exhibit germline cysts with germline-derived nurse cells and an oocyte surrounded by somatically-derived follicle cells (Figure 1H,J). In contrast, uninfected ovarioles exhibit an abundance of cysts either lacking the follicle cell exterior (Figure 1I) or the germline-derived interior (Figure 1K). These comparative data for a range of *mei-P26* alleles, RNAi-knockdowns, and host ages indicate that wMel rescues *mei-P26's* developmental functions in early host oogenesis. In contrast, wMel does not rescue *mei-P26*'s role in meiosis. Segregation defects were not rescued by wMel infection, as indicated by elevated X-chromosome nondisjunction (NDJ) rates in both infected and uninfected *mei-P26[1]* homozygous hypomorphs (NDJ = 7.7% and 5.6%, respectively, Figure S3A,B).

In the *D. melanogaster* germarium, wMel is continuously present at high titers in both germline and somatic cells (Figure 1L-M'), consistent with previous reports (*25*, *26*, *42*). The bacteria appear to localize more strongly to the germline-derived cells than the somatic cells in the germarium (co-localization of FtsZ and Vas in Figure1 L). Intracellular wMel can be identified in the GSC, the cystoblast, the cystocytes, and the developed cyst. This positioning puts wMel in all of the critical cell types and stages that *mei-P26* is active, enabling the bacterium to compensate for *mei-P26's* developmental functions in GSC maintenance and differentiation. In the following sections, we analyze wMel's ability to rescue *mei-P26* function at each of the critical timepoints in early oogenesis.

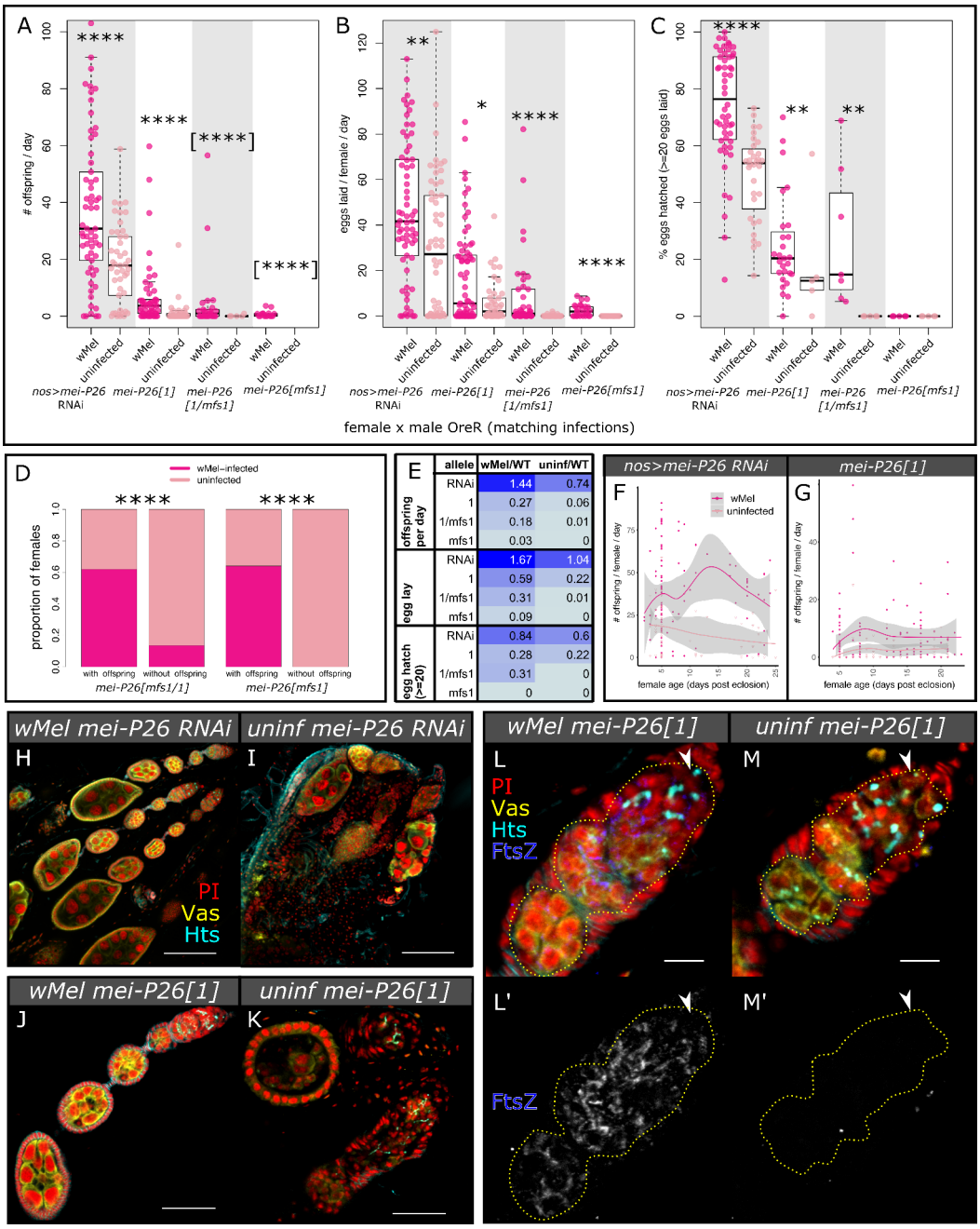

Figure 1. wMel infection rescues the loss of essential host fertility gene *mei-P26* in females (and males, see Figure S3E-G). A-C) Beeswarm boxplots of A) overall offspring production, broken into B) egg lay and C) egg hatch, in RNAi, hypomorphic, and null *mei-P26* knockdown female flies. The null allele *mei-P26[mfs1]* reduced egg lay numbers in both transheterozygotes and homozygotes below an average of 20 for both infected and uninfected females, necessitating an analysis of females with and without offspring (see Figure S3). Wilcoxon Rank Sum * = p<0.05, ** = 0.01, *** = 0.001, **** = 1e-4. Fisher's exact test [****] = p<1e-4. D-E) D) Bar plots of the proportion of female samples of the indicated genotypes with offspring and without offspring, infected and uninfected with *Wolbachia*. Fisher's exact test **** = p<1e-4. E) Table listing the proportion of wild-type fecundity demonstrated by wMel-infected (left) or uninfected (right) *mei-P26* mutants in order of increasing severity, from top to bottom (see also Table S1-3). Cells values from low to high proportions are colored from light to dark blue, respectively. F-G) Knockdown *mei-P26 D. melanogaster* fecundity vs. female age, fit with a local polynomial regression (dark gray bounds=95% confidence intervals). Infection with wMel enhances offspring production over the first 25 days of the (F) *mei-P26* RNAi and (G) *mei-P26[1]* hypomorphic female lifespan. H-M') Confocal mean projections of *D. melanogaster* ovarioles and germaria. H-K) Cytology reveals

that wMel-infection rescues H-I) *mei-P26* RNAi and J-K) *mei-P26[1]*-induced oogenesis defects. L-M') Intracellular wMel FtsZ localizes to germline (Vas+, outlined in dashed yellow) and somatic (Vas-) cells at high titers, with low background in uninfected flies. Bacteria are continuously located in the *mei-P26[1]* germline, starting in the GSC (arrowhead near Hts-bound spectrosome). Fluorescence channels were sampled serially and overlaid as indicated on each set of figures as follows: cyan=anti-Hu Li Tai Shao (Hts), yellow=anti-Vasa (Vas), blue=anti-Filamenting temperature-sensitive mutant Z (FtsZ), and red=propidium iodide (PI) DNA staining. Scale bars F,H = 100 μm, H,I = 50 μm, and J,K = 10 μm.

Host GSCs are maintained at higher rates in wMel-infected than uninfected mei-P26-deficient flies

GSCs were quantified by immunofluorescence staining of the essential GSC markers phosphorylated Mothers Against Dpp (pMad) and Hu Li Tai Shao (Hts). Staining revealed an increase in the average number of GSCs per *mei-P26[1]* germarium with wMel infection, relative to uninfected germaria (young/infected/hypomorph: 1.0 vs young/uninfected/hypomorph: 0.58, p=2.9e-4, Wilcoxon Rank Sum), but GSC maintenance did not reach wild-type rates (young/infected/WT: 2.3 and young/uninfected/WT: 1.9, uninfected, p=1.2e-4 to 2.8e-4, Wilcoxon Rank Sum; Figure 2A-E). wMel-infected *mei-P26[1]* germaria also had more cells manifesting other GSC properties, such as a large cytoplasm and physical attachment to the cap cells of the somatic niche (*43*), than uninfected germaria. In contrast to the *mei-P26[1]* allele, RNAi knockdown of *mei-P26* did not significantly affect the numbers of GSCs per germarium (infected/RNAi: 2.1 and uninfected/RNAi: 1.9; Figure 2E and S4A,B), suggesting that the modest reductions in *mei-P26* dosage have a stronger impact on differentiation than GSC maintenance. Wild-type germaria did not exhibit different numbers of GSCs due to wMel infection (Figure 2C-E). See Table S5 for all p-values.

The number of GSCs per germarium in wMel-infected *mei-P26[1]* females converges on wild-type values in older germaria (Figure S4C). As wild-type flies age, the number of GSCs per germarium declines naturally (*44*), even in wMel-infected flies (aged/infected/WT: 1.6 vs. young/infected/WT: 2.3, p=0.019, Wilcoxon Rank Sum). Both infected and uninfected *mei-P26[1]* females appear to recover some of their GSCs as they age (aged/infected/hypomorph: 1.5 and aged/uninfected/hypomorph: 0.94, p=0.013-0.014, Wilcoxon Rank Sum). While wild-type OreR infected and uninfected flies lose from 3% to 31% of their GSCs in the first two weeks, infected and uninfected *mei-P26[1]* flies increase their GSC abundance by 43% and 63% in this time. Taking both age-dependent trajectories in GSC retention into account, by the time wMel-infected *mei-P26[1*] germaria are 10 days old, they contain the same average number of GSCs per germarium as wild-type flies and significantly more GSCs than uninfected *mei-P26[1]* flies (p=0.015, Wilcoxon Rank Sum; Figure S4C). Therefore, *Wolbachia* enhances stem cell maintenance in both young and old *mei-P26[1]* females.

Infected *mei-P26[1]* GSCs are functional, as indicated by their ability to undergo mitosis (Figure 2F-J, Table S6). We identified nuclei in mitosis by positive anti-phospho-histone H3 (pHH3) staining, a specific marker of Cdk1 activation and mitotic entry (*45*). Significantly fewer GSCs were in mitosis in uninfected *mei-P26[1]* germaria than infected *mei-P26[1]* and uninfected wild-type OreR germaria (0.09% vs 6%, p=4.7e-2 and 4.6e-2 Fisher's Exact Test; Figure F,G,J). There was no difference in the frequency of GSCs in mitosis between uninfected and infected wild-type germaria (5-6%, Figure H-J). Mitotic cystoblasts and cystocytes were only significantly enriched in infected *mei-P26[1]* germaria compared to infected wild-type germaria (p=1.3e-2 Wilcoxon Rank Sum; Figure S4D, Table S7), despite over-replication during transit-amplifying (TA) mitosis being a common phenotype in uninfected *mei-P26[1]* germaria (discussed below and (*46*)).

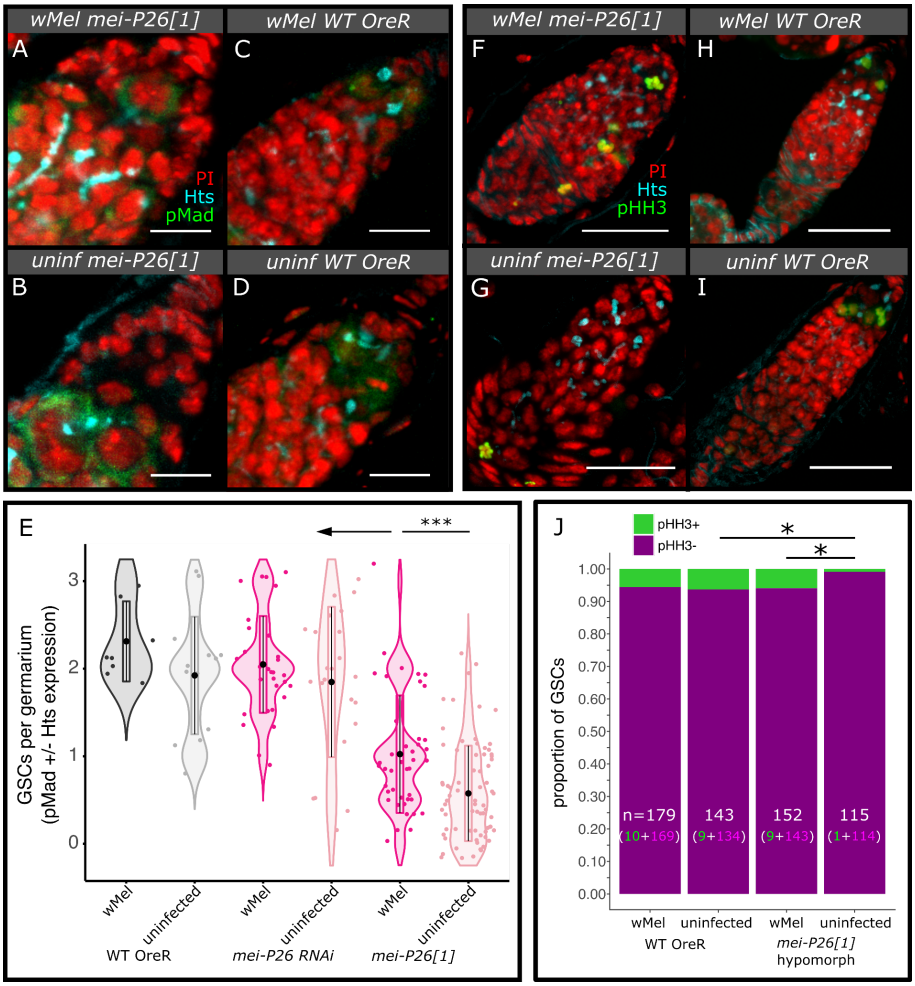

Figure 2. wMel infection rescues *mei-P26*-induced defects in female germline stem cell (GSC) maintenance. A-E) Infection with wMel confers higher numbers of GSCs per germarium in *mei-P26[1]* flies than in uninfected. A-D) Confocal mean projections of *D. melanogaster* germaria stained with antibodies against Hts and pMad. E) Violin plots of the number of GSCs per germarium. As fully functional GSCs express pMad and have Hts-labeled spectrosomes, each was weighted by half and allows for partial scores. Wilcoxon Rank Sum * = p<0.05, ** = 0.01, *** = 0.001, **** = 1e-4. F-J) We detected mitotic GSCs by pHH3 expression, finding that wMel restored mitosis in hypomorphic *mei-P26* GSCs relative to uninfected GSCs. F-I) Confocal mean projections of *D. melanogaster* germaria stained with antibodies against Hts and pHH3. J) Stacked bar chart of the proportion of GSCs found expressing pHH3 in female germaria. Fisher's Exact Test *=p<0.05. Fluorescence channels were sampled serially and overlaid as indicated on each set of figures as follows: cyan=anti-Hts, yellow=anti-Vas, red=PI, green=anti-pMad in A-D and anti-pHH3 in F-I. Scale bars A-D = 10 μm and F-I = 25 μm.

Regulation of host Sxl expression is rescued in wMel-infected germaria

Proper Sxl expression is required for GSC maintenance and differentiation (*47*). High levels of Sxl in the GSC maintains stem cell quiescence (*48*). When the GSC divides and the cystoblast (CB) moves away from the niche, Sxl cooperates with Bam and Mei-P26 to bind to the *nos* 3' untranslated region (UTR) and downregulate Nos protein levels to promote differentiation (*46*, *49*).

Loss of *mei-P26* dysregulates Sxl expression in uninfected flies, which is mitigated by wMel infection. Less Sxl is expressed in uninfected *mei-P26[1]* germarium region 1 and more Sxl is expressed across regions 2a and 2b, relative to wild-type (p=5.7e-10 to 5.3e-5 pairwise Wilcoxon Rank Sum; Figure 3 and S4E, Table S8).

Infection with wMel increased Sxl expression in germarium region 1 and suppressed expression across regions 2a and 2b relative to uninfected *mei-P26[1]*, replicating an expression pattern similar to that seen in wild-type germaria (p=5.7e-10 to 8.4e-3, Wilcoxon Rank Sum). These results suggest that wMel's mechanism for *mei-P26* rescue may also explain how Sxl's Nos-repressing function in the CBs is rescued by wMel infection (*30*, *33*).

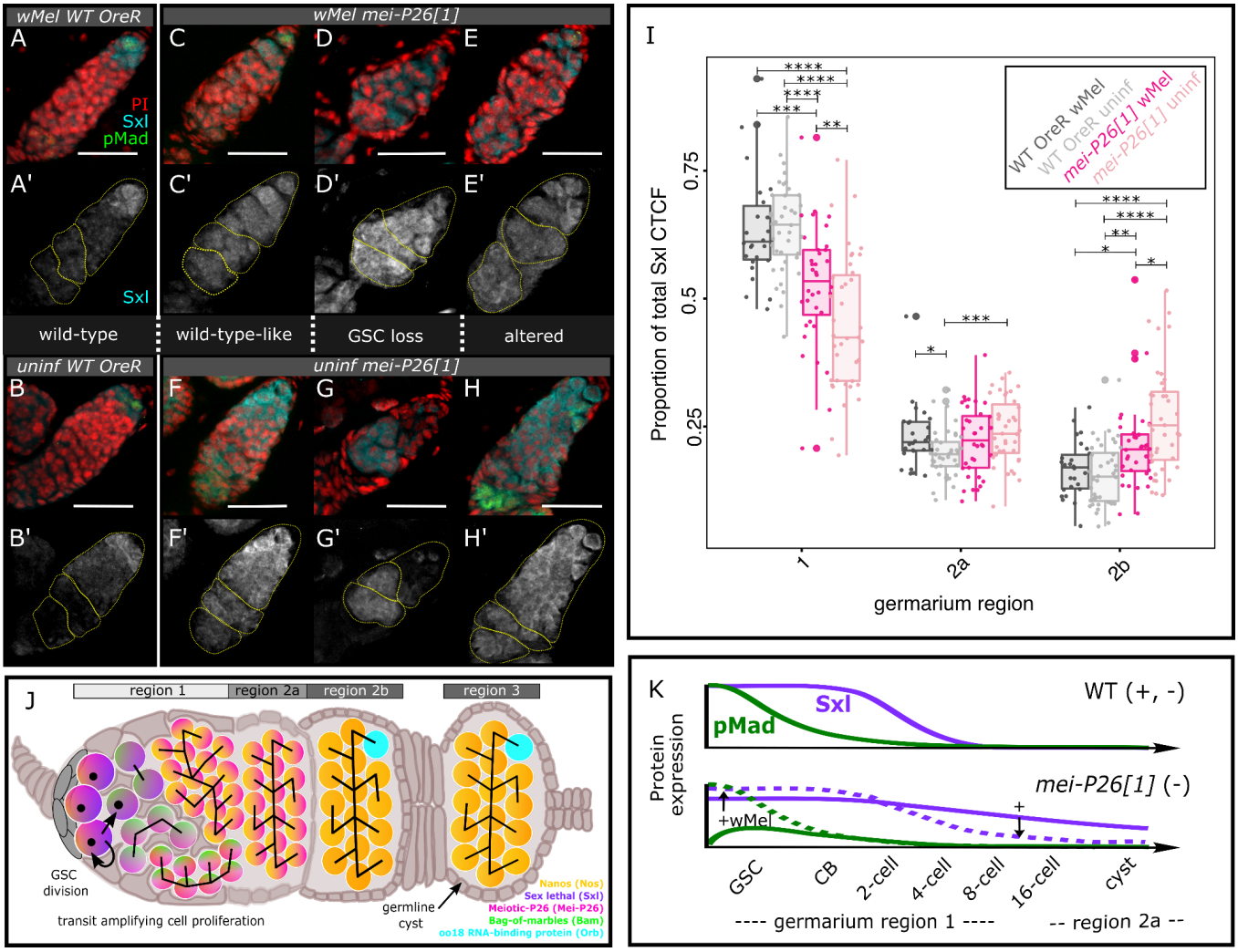

Figure 3. Infection with wMel mitigates the consequences of dysfunctional *mei-P26* on *Sxl* expression in the germarium. A-H') Confocal mean projections of *D. melanogaster* germaria stained with antibodies against Sxl and pMad. Three phenotypes for each *mei-P26[1]* infection state are shown, (left) one as similar to wild-type as possible, (middle) one representative of GSC loss, pMad-negative, and (right) one representative of a developmentally altered phenotype retaining pMad-positive GSCs. We sampled the fluorescence channels serially and overlaid them as indicated on each set of figures: cyan=anti-Sxl, red=PI, green=anti-pMad. Scale bars = 25 μm. I) Bar-scatter plots of relative Sxl fluorescence expression levels across the germarium, by region. Colors as labeled in Figures 1A-D and 2E, from left to right: wild-type OreR in gray, dark gray = wMel-infected and light gray = uninfected; *mei-P26[1]* hypomorphs in pink, dark pink = wMel-infected and light pink = uninfected. Wilcoxon Rank Sum * = p<0.05, ** = 0.01, *** = 0.001, **** = 1e-4. J) Diagram of a *D. melanogaster* germarium, highlighting key events and cell types by region as in (*50*). Somatic cells in beige, GSC-derived cells are brightly colored gradients leading to differentiated cyst cells in yellow, with specified oocytes in blue. The black structure that originates in the GSC is the spectrosome, which becomes a branching fusome as the CB is formed, moves away from the niche, and divides. K) Model of wMel Sxl expression rescue

in *mei-P26[1]* germaria. Green dashed line represents wMel's upregulation of pMad expression in the GSC (Figure 2A-E). Purple dashed line represents wMel's upregulation of Sxl in the GSC/CB and downregulation of Sxl in germarium region 2a. Arrows with + symbols indicate wMel's action on gene expression.

Bam expression is partially restored in wMel-infected mei-P26 mutant germaria

In wild-type female flies, Bam expression begins immediately after the cystoblast daughter cell moves away from its undifferentiated sister, which remains bound to the GSC niche ((*46*, *51*) and illustrated in Figure 3J, Bam in green). Bam binds to the fusome and stabilizes CyclinA to promote TA mitosis, producing 16 cyst cells from a single CB (*52*).

Loss of Mei-P26 deregulates and extends Bam expression, producing excess nurse cells (*46*), as seen in *mei-P26[1]* germaria (Figure 4, S4F, and Table S9). Bam dysregulation in *mei-P26[1]* germaria is mitigated by wMel infection (Figure 4C,D vs E,F). Infection with wMel mitigates the impacts of Mei-P26 loss, inducing Bam expression to rise rapidly from a low level in the GSCs and fall rapidly in the posterior 2a region, coincident with the 8-cell cyst stage, similar to wild-type (Figure 4G). Whereas, without wMel, *mei-P26[1]* germaria produce lower peak Bam expression than infected and wild-type at the CB-to-16-cell stage (p=0.02 and 0.03, Wilcoxon Rank Sum), and higher Bam expression than wild-type in germarium regions 2a and 2b (p=0.02-0.04, Wilcoxon Rank Sum).

Both infected and uninfected *mei-P26[1]* germaria exhibit lower Bam expression than wild-type in the GSC niche, in contrast to expectations, but consistent with a loss of true pluripotent GSCs. In the GSC, bone morphogenic protein (BMP) signaling from the somatic niche induces pMad expression, which directly represses Bam transcription, preventing differentiation (*53*). Loss of mei-P26 function in the GSC should derepress Brat, resulting in pMad repression, and inappropriate Bam expression (*36*). However, we see lower Bam expression in both wMel-infected and uninfected *mei-P26[1]* GSCs relative to wild-type (p=1.3e-6 to 1.4e-3, Wilcoxon Rank Sum; Figure 4G). The elevated relative Bam/pMad expression ratio in uninfected *mei-P26[1]* GSCs (p=2.5e-4 to 4.0e-4, Wilcoxon Rank Sum; Figure 4H and Table S10) may explain this departure from expectations. Although Bam expression is lower than in wild-type, Bam expression is clearly dysregulated and upregulated relative to pMad expression, as expected for germline cells that have lost their stem cell identity (*54*, *55*). Figure 4G suggests that wMel may elevate Bam expression even higher than wild-type levels in *mei-P26[1]* hypomorphs at the CB-to-16-cell stage, and normalizing against pMad expression confirms this (p=1.2e-6 to 2.0e-2, Wilcoxon Rank Sum). Thus, wMel both elevates and suppresses Bam expression at the proper timepoints in *mei-P26[1]* flies to achieve an expression profile similar to wild-type during early oogenesis (Figure 4I).

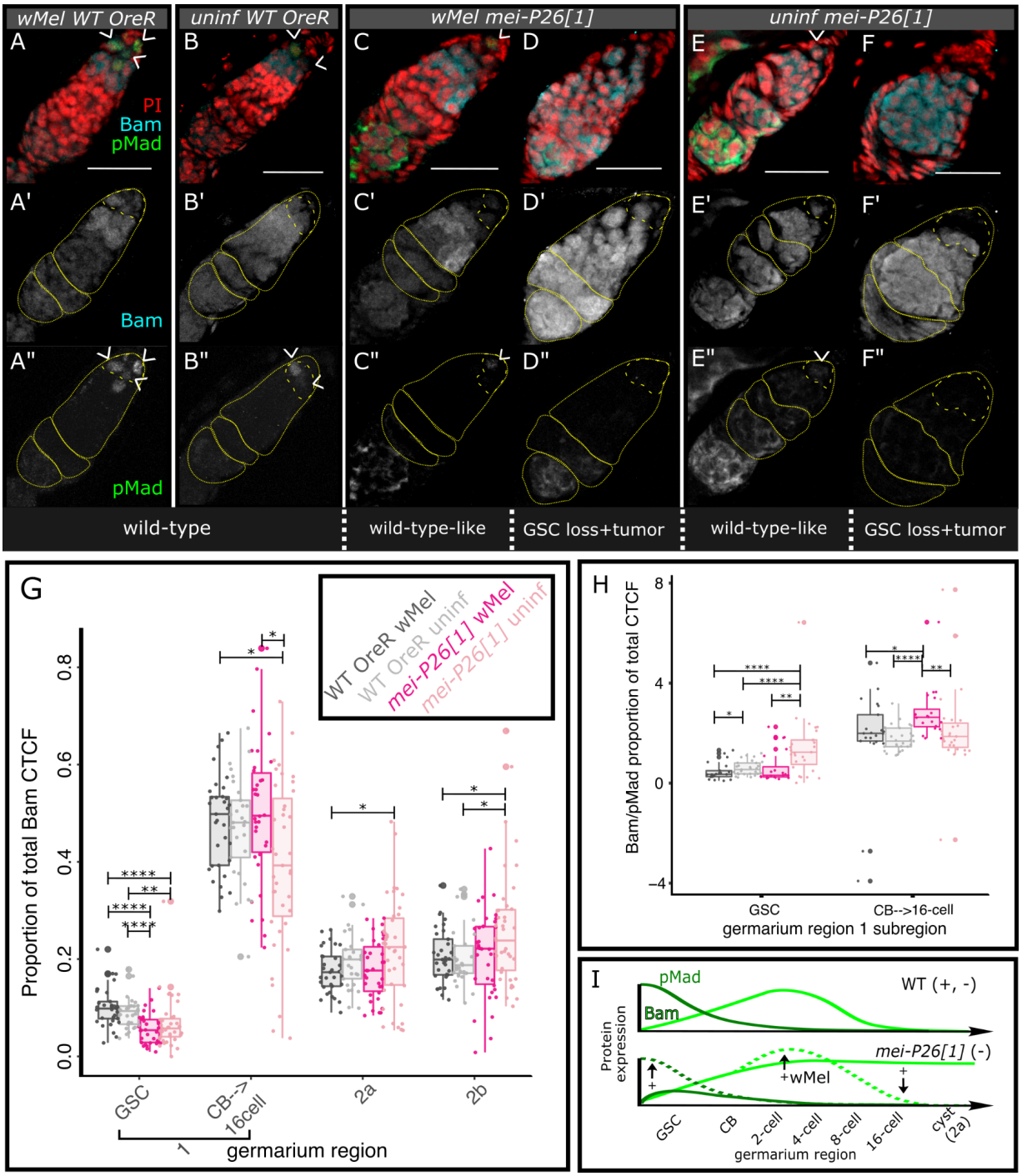

Figure 4. Infection with wMel mitigates the consequences of dysfunctional *mei-P26* on *Bam* expression in the germarium. A-F") Confocal mean projections of *D. melanogaster* germaria stained with antibodies against Bam and pMad. Two phenotypes for each *mei-P26[1]* infection state are shown, (left) one as similar to wild-type as possible and (right) one representative of developmentally altered phenotypes. G) Bar-scatter plots of relative Bam fluorescence expression levels across the germarium, by region. Bam expression ramps up in the CB , so we subdivided region 1 into GSC and CB/cystocyte subsections. H) Bar-scatter plot of the ratio of relative Bam to pMad fluorescence. As pMad and Bam are mutually exclusively expressed in the GSC and CB/cystocytes, respectively, wild-type values are near zero. Values significantly higher than this reflect dysregulation of the stem cell state. I) Model of wMel rescue of Bam expression in *mei-P26[1]* germaria. Colors as labeled in Figures 1A-C, 2E, and 3G-H, from left to right: wild-type OreR in gray, dark gray = wMel-infected and light grey = uninfected; *mei-P26[1]* hypomorphs in pink, dark pink = wMel-infected and light pink = uninfected. Wilcoxon Rank Sum * = p<0.05, ** = 0.01, **** = 1e-4. Scale bars = 25 μm.

wMel rescues normal germline cyst and oocyte development impared by *mei-P26* knockdown

Over-proliferated nurse cells and partially-differentiated GSCs combine to produce tumorous germline cysts in Mei-P26-deficient flies ((*36*, *37*) and Figure 5A-D vs E-H). In RNAi knockdown ovaries, the formation of tumorous germline cysts is significantly mitigated by wMel infection (35.3% vs 16.3% of cysts with more than 15 nurse cells, respectively; p=4.5e-3, Fisher's Exact Test; Figure 5E-F vs G-H). In contrast, germline cyst tumors found in *mei-P26[1]* allele germaria were not rescued by wMel infection, despite the bacterium's ability to rescue the rate at which these eggs hatch into progeny (Figure 5I vs 1A,C). The stronger nature of the *mei-P26[1]* allele relative to the nos-driven RNAi knockdown likely underlies the difference in the number of tumorous cysts. Lack of tumor rescue indicates that either tumorous cysts produce normal eggs at some rate or wMel infection rescues tumors at a later point in oogenesis, perhaps through some somatic mechanism (*56*–*59*).

While overexpression of *mei-P26* produces tumors in both uninfected and infected ovaries, infected ovaries exhibit significantly more tumors than wild-type (p=1.6e-3, Fisher's Exact Test; Figure 5I, Table S11). To elucidate the interaction between *mei-P26* and wMel, we overexpressed *mei-P26* in infected and uninfected backgrounds and evaluated the impact on the formation of germline tumors. This dominant-negative type of interaction suggests a wMel-encoded factor acts to enhance Mei-P26 function, potentially through direct interaction or a redundant function. Given that tumorous cysts consist mostly of cells with nurse cell-like nuclei in dosage defective flies (Figure 5E-H), the differences among these tumor phenotypes are likely due to differential regulation of the transit-amplifying mitoses that populate 15-nurse cells and one oocyte in the germline cyst, opposed to an accumulation of undifferentiated stem-like cells. If true, this would support our finding that wMel restores the downregulation of Bam during the TA mitoses that pattern the cyst (Figure 4).

Oocyte specification in region 2a of the germarium is inhibited by the loss of *mei-P26* through the derepression of *orb* translation (*36*), and wMel infection increases the rate of oocyte-specific Orb translation (Figure 5J-R). Mei-P26 regulates Orb expression by binding to the *orb* 3' UTR and preventing its translation. Following cyst patterning and development, one of the 16 germline-derived cells is designated as the oocyte through specific oo18 RNA-binding protein (Orb) expression (*60*). In region 2a, the germline cyst cell fated to become the oocyte activates *orb* translation (*36*). Loss of *mei-P26* results in *orb* derepression and non-specific expression (*36*). Infection with wMel restores oocyte-specific Orb expression in *mei-P26[1]* cysts relative to uninfected cysts (p=5.9e-9, Fisher's Exact Test; Figure 5L-N vs O-Q). We observed oocyte-specific Orb staining 93-94% of the time in wild-type cysts, whereas *mei-P26[1]* reduced this frequency to 25%, and wMel infection recovered *mei-P26[1]* cysts to 61% (counts in Table S12). Oocyte-specific expression of Orb in wMel-infected cysts is robust, even in those that are developmentally aberrant (*e.g.*, the double oocyte in Figure 5M). These results suggest that wMel recapitulates oocyte-specific Orb translation enhancing or duplicating Mei-P26's function in *orb* translational repression.

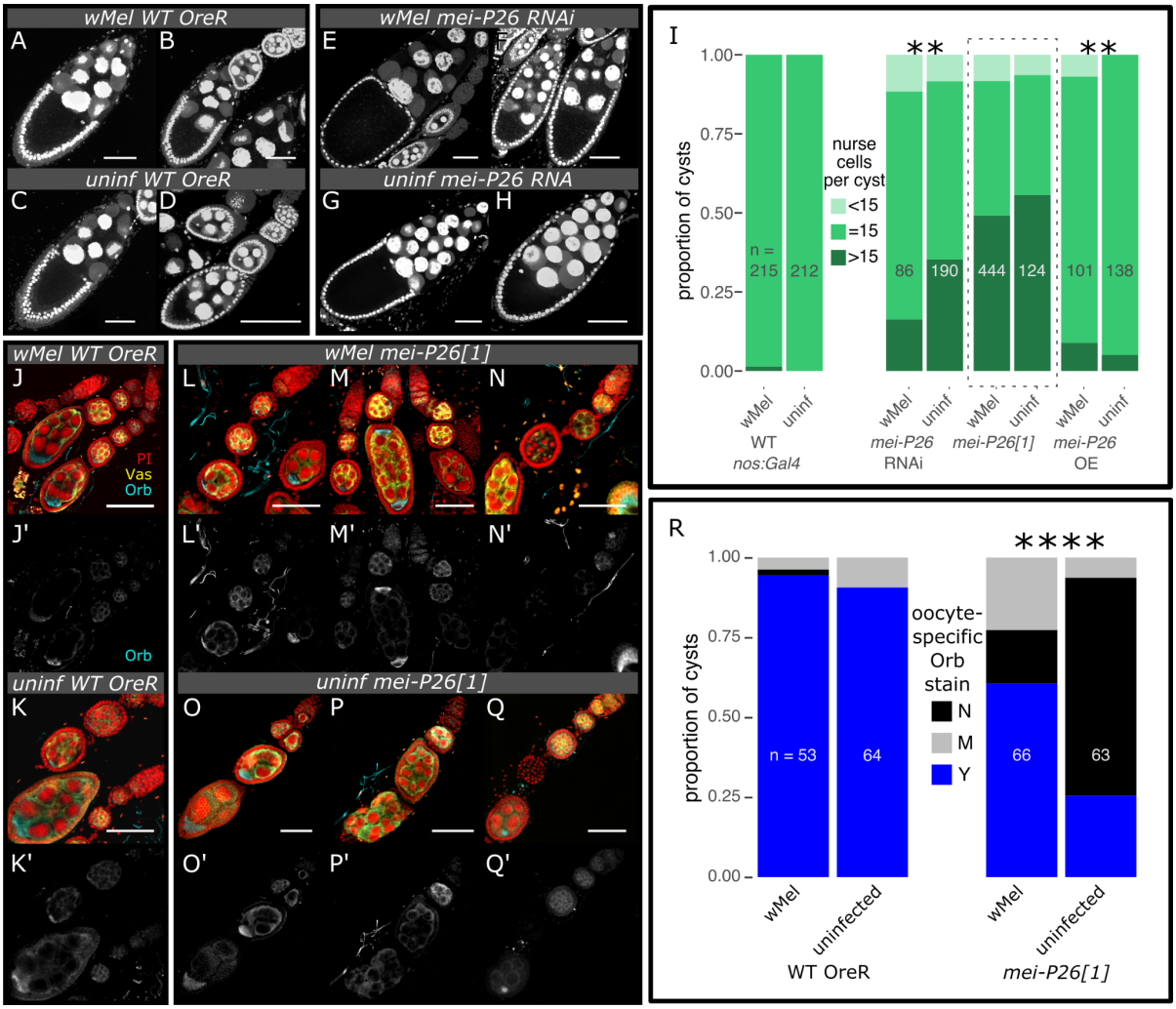

Figure 5. wMel infection rescues cyst tumors and restores oocyte specification in *mei-P26* mutants. A-I) Loss and over-expression of Mei-P26 induces the formation of tumorous cysts, which contain more than 15 nurse cells. wMel infection mitigates *nos*>RNAi-knockdown and exacerbates *nos*>overexpression (OE) phenotypes. A-H) Confocal max projections of ~25 µm-thick sections of *D. melanogaster* oocyte cysts stained with PI. I) Stacked bar chart of the proportion of germline cysts containing an abnormal number of nurse cells (less than or greater than 15 nurse cells). J-R) Hypomorphic *mei-P26[1]* cysts infected with wMel significantly restored Orb translational regulation relative to uninfected cysts. Oocyte specification occurs in regions 2b-3 of the germarium (see diagram in Figure 3J), when Orb expression becomes restricted to the nascent oocyte. J-Q') Confocal mean projections of *D. melanogaster* germaria stained with antibodies against Orb and Vas. R) Stacked bar chart of the proportion of germline cysts containing oocyte-specific Orb staining. Sample sizes are written on the bar charts. N=no, M=maybe, and Y=yes. Fisher's Exact ** = p<1e-2, **** = p<1e-4. Scale bars = 50 µm.

Wild-type host fertility is beneficially impacted by wMel infection

Consistent with wMel's ability to rescue the partial to complete loss of essential germline maintenance genes encompassing a range of functions, we discovered that this intracellular symbiont enhances wild-type *D. melanogaster* fertility (Figure 6A-C, S5A-D, Table S1-3). We analyzed egg lay, egg hatch, and offspring production rates independently to detect wMel effects on multiple components of fecundity. Infection with wMel increased the number of eggs laid per female per day for the nos:Gal4/CyO balancer wild-type stock by 49% (42 vs 28 eggs/female/day, p=2.2e-3, Wilcoxon Rank Sum), but did not have any detectable effect on wild-type

genotypes. Following embryogenesis, infection with wMel elevates the rate that OreR and nos:Gal4/CyO wild-type eggs hatch into L1 stage larvae by 2.8-9.3% (88-91% vs. 81-89% of eggs hatched, p=<1e-4 to 2.1e-3, Wilcoxon Rank Sum). Overall offspring production per female per day was elevated in wMel-infected nos:Gal4/CyO females relative to uninfected females by 49% (40 vs. 27 offspring/female/day, p=2.2e-3, Wilcoxon Rank Sum). These results suggest that beneficial impacts of wMel infection are evident, yet variable among wild-type *D. melanogaster* stocks.

We measured OreR fertility across its lifetime (~50 days), and found that wMel's enhancement of egg hatch is maintained (p=7.1e-9 Kolmogorov-Smirnov Test; Figure 6B). As OreR females age, wMel infection may maintain higher rates of egg production (Figure S5D), culminating in age ranges in which infected flies produce an excess of offspring relative to uninfected (~20-30 days old; Figure 6C), although the overall differences in fecundity curves are insignificant (Table S4). Intriguingly, the wMau strain from *Drosophila mauritania* also elevates host egg production by increasing GSC proliferation (*25*), implying that this may be a common mechanism underlying *Wolbachia's* success.

Immunostaining of anti-FtsZ confirms that wMel exhibits high titers in the wild-type germarium and concentrates in the oocyte in early cysts (Figure 6D-F'). The intracellular bacteria are continuously located in the germline, starting in the GSC. Thus, wMel are located in the right place at the right time to enhance female host fertility, as well as to correct for perturbations caused by male CI-related alterations (*61*).

The wMel strain of *Wolbachia* in its native *D. melanogaster* host exhibits weak CI that decreases with age (Figure 6G-H, S6A-D), suggesting low maintenance of CI mechanisms (*8*). Mating wMel-infected OreR males to infected and uninfected OreR virgin females revealed that wMel reduces uninfected egg hatch by 26% when males are zero to one day old (p=4.6e-4, Wilcoxon Rank Sum), but this moderate effect is eliminated by the time males are five days old. In contrast, the *Wolbachia* wRi strain that naturally infects *Drosophila simulans* and induces strong CI (*10*, *62*), reduces uninfected egg hatch by 95% when males are zero to one day old (p=5.6e-8, Wilcoxon Rank Sum) and only loses some of this efficacy by five days (75% hatch reduction, p=3.6e-4, Wilcoxon Rank Sum; Figure S6E-H). Overall, these results suggest that wMel's beneficial reproductive manipulations may affect its fitness more than its negative reproductive manipulations in nature.

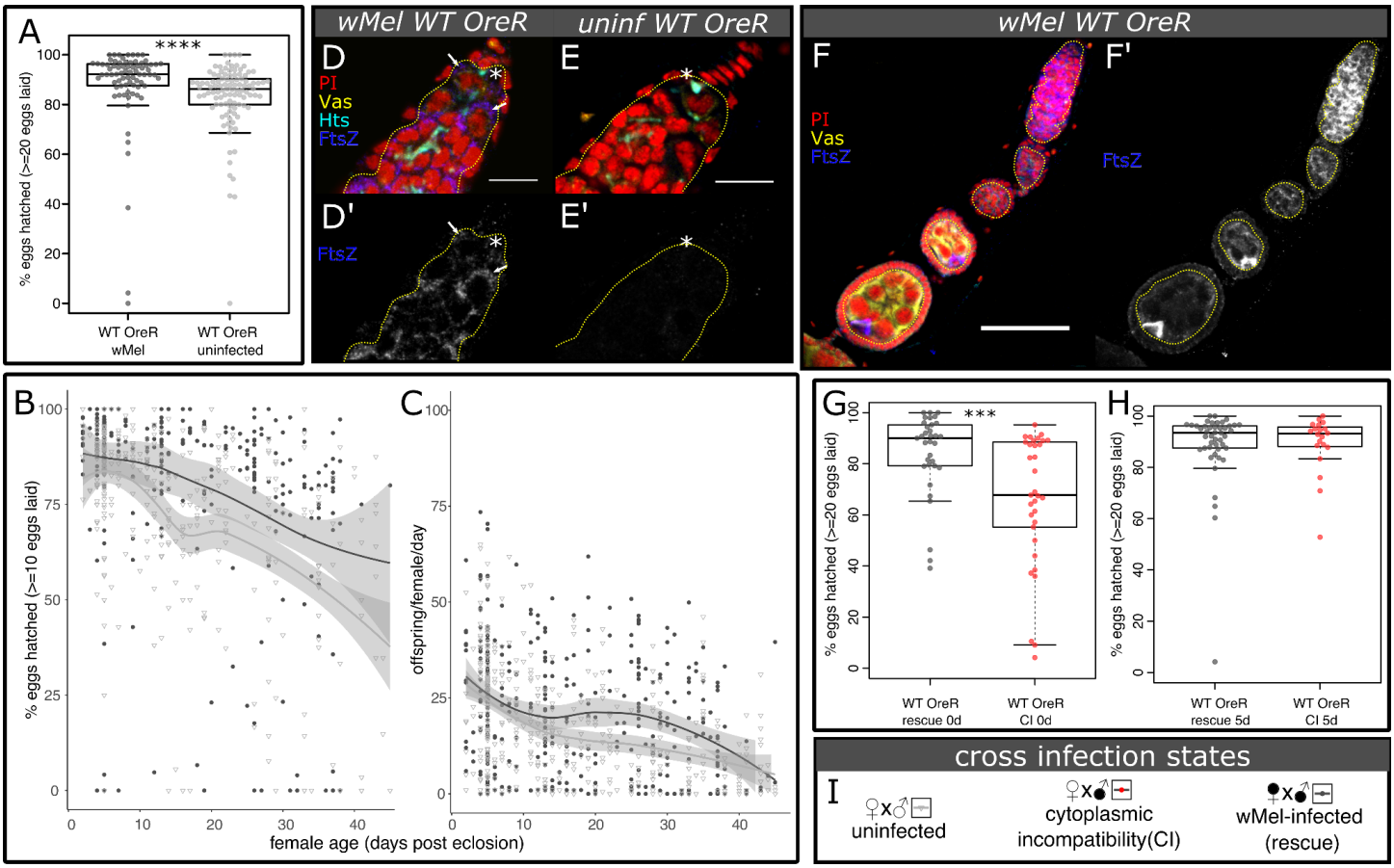

Figure 6. The wMel strain of *Wolbachia* is a beneficial manipulator of host reproduction. A) Beeswarm boxplot showing that wMel infection elevates the hatch rate of wild-type *D. melanogaster* OreR eggs relative to uninfected flies of the same genotype by 5.2%. B-C) *D. melanogaster* fecundity vs. female age, fit with a local polynomial regression (dark gray bounds = 95% confidence intervals). Infection with wMel elevates B) egg hatch rate and C) offspring production across the host lifespan. D-F') Confocal mean projections of *D. melanogaster* D-D') infected and E-E') uninfected germaria and F-F') an infected ovariole. Intracellular wMel FtsZ localizes to germline (Vas+, outlined in dashed yellow) and somatic (Vas-) cells at high titers in infected wild-type flies, with low background in uninfected flies. Bacteria in the GSC (* near the Hts-bound spectrosome) are indicated with an arrow. Fluorescence channels were sampled serially and overlaid as indicated on each set of figures as follows: cyan=anti-Hts, yellow=anti-Vas, blue=anti-FtsZ, and red=PI. Scale bars F-G = 10 μm, H = 50 μm. G,H) Beeswarm boxplots of the proportion of eggs that hatch when infected males are mated to uninfected or infected OreR females reveal that wMel evokes G) weak CI when males are 0-1 days old and H) no CI by the time males are 5 days old. I) Key to fecundity cross infection states, terms, colors, and symbols for A-C,G,H. Wilcoxon Rank Sum *** p< 0.001, **** < 1e-4.

Discussion

The wMel strain of *Wolbachia* is a successful and widespread symbiont: naturally in *D. melanogaster* populations and novelly through lab-generated trans-infections of wMel into non-native hosts used for biological control. However, we know remarkably little about the processes that shape how symbiont and host co-evolve and find mutually beneficial mechanisms for their reproduction. In this work, we confirm that wMel's CI strength is typically weak in *D. melanogaster,* (Figure 6G-H, (*14–18*)) and show that wMel confers benefits on host fertility (Figures 1-5 and 6A-F).

Here, we demonstrate that wMel infection can elevate host fitness in both wild-type and *mei-P26* mutants, and we shed light on the long-standing mystery of how wMel beneficially impacts host reproduction. Previously, wMel was shown to rescue the loss of Sxl (*30*) and Bam (*31*), two essential genes for two very different stages of early oogenesis: GSC maintenance/CB differentiation and TA-mitosis, respectively. These findings left unresolved how wMel suppresses these mechanistically and temporally distinct phenotypes. Here, we show that infection with wMel rescues defects associated with mutant *mei-P26,* a gene required for both GSC maintenance and differentiation. Infection with wMel rescues all stages of oogenesis in *mei-P26* RNAi knockdowns, as well as hypomorphic and null alleles (Figures 1-5). Mei-P26 is a TRIM-NHL protein that regulates gene expression via mRNA translational inhibition through the Nos mRNA-binding complex, interactions with the RNA-induced silencing complex (RISC), and protein ubiquitination (*36*, *63*). Importantly, Mei-P26 interacts with Sxl in the GSC and CB and Bam in the CB and cystocytes (*35*, *46*). These interactions suggest that the mechanism wMel employs to rescue mei-P26 function may also be responsible for rescuing aspects of Sxl-dependent GSC maintenance and CB differentiation and Bam-dependent cyst differentiation.

In this first in-depth molecular and cellular analysis of wMel-mediated manipulation of GSC maintenance and differentiation, we discovered that wMel rescues *mei-P26* germline defects through restoring pMad, Sxl, Bam, and Orb gene expression to approximately wild-type levels (diagrammed in Figure 7A). Infection with wMel partially rescued GSC-specific pMad expression relative to wild-type levels (Figure 2A-E), suggesting that the bacteria restored BMP signaling from the niche (*36*). Finding that these cells are also able to divide (Figure 2F-J), further supports their functionality and stemness. Given that *mei-P26* is likely involved in *Drosophila* Myc (dMyc) regulation, and overexpression of dMyc induces competitive GSCs (*64*), wMel's GSC rescue mechanism may involve dMyc upregulation. In the germline cells that left the niche, wMel recapitulated the properly timed changes in pMad, Sxl, and Bam expression that are normally influenced by *mei-P26* and are required during cystoblast differentiation to form the 16-cell germline cyst (*37*, *38*, *46*, *63*) (Figures 3-4, S4E,F).

This is the first time wMel has been found to rescue oocyte differentiation post-cyst formation, suggesting that wMel has pervasive impacts throughout oogenesis. We confirmed the downstream consequences of Bam rescue by finding fewer germline cyst tumors in infected flies (Figure 5A-I). These germline cysts appeared to be functional, based on restored oocyte-specific expression of the essential oocyte differentiation protein Orb in infected *mei-P26[1]* cysts, relative to uninfected cysts (Figure 5J-R).

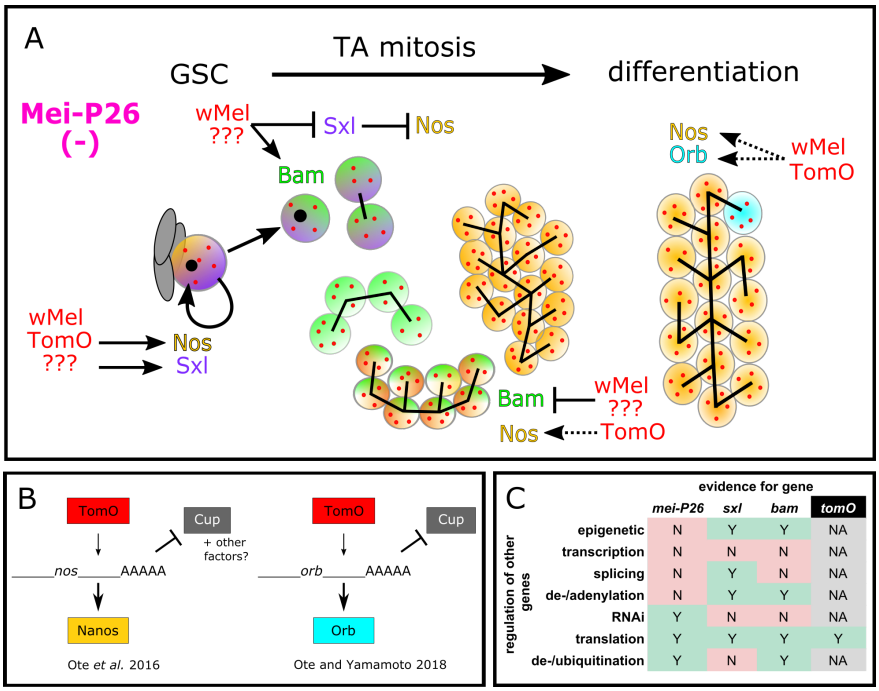

C

regulation of other genes	evidence for gene: *mei-P26*	*sxl*	*bam*	*tomO*
epigenetic	N	Y	Y	NA
transcription	N	N	N	NA
splicing	N	Y	N	NA
de-/adenylation	N	Y	Y	NA
RNAi	Y	N	N	NA
translation	Y	Y	Y	Y
de-/ubiquitination	Y	N	Y	NA

Figure 7. Model of wMel's interactions with essential host genes in early GSC maintenance and germline cyst formation. A) In *mei-P26* mutants, wMel restores normal Bam, Sxl, and Orb expression through various mechanisms, most of which are unknown (??? = unknown wMel factor(s)). Expression rescue correlates well with cytological rescue from GSC maintenance through germline cyst differentiation. B) Sxl rescue in the GSC is mediated through TomO's interaction with RNPs containing *nos* mRNA, upregulating Nos translation. Later, in stage 8 of cyst oogenesis, TomO was found to bind *orb* mRNA, displacing the translational repressor Cup, and upregulating Orb translation (*33*, *34*). Dashed arrow in A indicates TomO's predicted function in enabling Orb derepression in early cyst differentiation. The factor that restores *mei-P26* repression of Orb translation in *mei-P26* mutants has not been identified. C) Table of gene regulatory functions reported for each host (black text) and wMel (white text) gene. See Table S13 for annotated table references.

The wMel strain's rescue of *D. melanogaster mei-P26* is likely independent of the *Wolbachia* TomO protein. Prior work on TomO indicates that the bacterial protein's primary mode of action is through destabilizing ribonucleoprotein (RNP) complexes (*34*) (diagrammed in Figure 7B,C). This is how TomO elevates Nos expression in the GSC (*33*) and how TomO inhibits the translational repressor Cup from repressing Orb translation in mid-oogenesis (stage 8) (*34*, *65*). In contrast, Mei-P26 interacts with Ago1 RISC to inhibit Orb translation through binding the *orb '3-UTR miRNA* binding sites (*36*). Although Mei-P26 and TomO produce opposite outcomes for Orb expression, TomO-*orb* binding may underlie wMel's ability to rescue Orb repression, if wMel produces other factors that modulate the interaction. Alternatively, wMel may make another RNA-binding protein. Given that Sxl is also repressed through the *sxl* 3'-UTR by Bruno (*66*), such a protein could be involved in restoring Sxl regulation in *mei-P26* mutants.

Additional bacterial factors besides TomO must be involved in reinforcing host fecundity in wild-type flies and fertility mutants. First, Mei-P26 encodes three functional domains that confer at least three different functional mechanisms for modulating gene expression (mRNA-binding, miRNA-mediated, and ubiquitination). In a bacterial genome, these domains/functions are likely to be encoded by more than one protein (*67*). Second, TomO rescues Sxl's GSC maintenance functions by binding *nos* mRNA, increasing levels of Nos translation, but it cannot fully rescue Sxl loss (*33*). Immediately after the GSC divides to produce the CB, Sxl interacts with Bam, Mei-P26, Bgcn, and Wh to inhibit Nos translation (*35*, *63*). Thus, a wMel factor that inhibits Nos

translation, counteracting TomO's function to destabilize Nos translational repressors through RNA-binding (*33*, *34*), remains to be identified. Furthermore, Nos upregulation cannot explain Bam rescue because Nos and Bam exhibit reciprocal expression patterns during TA mitosis (*35*). Third, exacerbation of the tumor phenotype induced by *nos*-Gal4-driven Mei-P26 overexpression by wMel infection (Figure 5I) suggests that wMel synthesizes a protein that directly mimics Mei-P26's functions in differentiation, and can reach antimorphic levels. Misregulated expression of a *mei-P26*-like factor could explain why wMel-infected *mei-P26* RNAi females produce more eggs and offspring than wild-type flies (Figure 1A,B). While TomO may recapitulate some of Mei-P26's functions, such as *orb*-binding, at least one other factor is needed to recapitulate proper Orb, Nos, and Bam regulation.

Understanding how *Wolbachia* interacts with host development at the molecular level is essential to deploying these bacteria in novel hosts and relying on vertical transmission to maintain them in host populations. CI has been a powerful tool for controlling host populations (*68*) and driving *Wolbachia* to high infection frequencies (*3*). Given that selection will favor the loss of CI if beneficial impacts on host fertility are realized (*8*), it is imperative that we understand the mechanisms underlying beneficial reproductive manipulations such as fertility reinforcement.

Acknowledgements: We thank the UCSC Life Sciences Microscopy Center (RRID:SCR_021135) and Ben Abrams for training and the use of their microscopes and Irene Newton for aliquots of anti-*Wolbachia* FtsZ antibodies. We thank Russ Corbett-Detig for his comments and feedback throughout this project. This work was supported by UC Santa Cruz and the NIH (R00GM135583 to SLR; R35GM139595 to WTS).

Author Contributions:
SLR, study conception and design, data production and analysis, and writing. JRC, data production and analysis, and writing. WTS, study design and writing.

References:

1. P. T. Leftwich, M. P. Edgington, T. Chapman, *Proc. R. Soc. B Biol. Sci.* **287**, 20200820 (2020).
2. M. Bright, S. Bulgheresi, *Nat. Rev. Microbiol.* **8**, 218–230 (2010).
3. A. Utarini *et al.*, *N. Engl. J. Med.* **384**, 2177–2186 (2021).
4. D. M. Drown, P. C. Zee, Y. Brandvain, M. J. Wade, *Evol. Ecol. Res.* **15**, 43 (2013).
5. M. R. Doremus, M. S. Hunter, in *Advances in Insect Physiology* (Elsevier, 2020; https://linkinghub.elsevier.com/retrieve/pii/S0065280620300035), vol. 58, pp. 317–353.
6. J. H. Werren, L. Baldo, M. E. Clark, *Nat. Rev. Microbiol.* **6**, 741–751 (2008).
7. V. A. A. Jansen, M. Turelli, H. C. J. Godfray, *Proc. R. Soc. B Biol. Sci.* **275**, 2769–2776 (2008).
8. M. Turelli, *Evolution*. **48**, 1500 (1994).
9. A. R. Weeks, M. Turelli, W. R. Harcombe, K. T. Reynolds, A. A. Hoffmann, *PLoS Biol.* **5**, e114 (2007).
10. L. B. Carrington, J. R. Lipkowitz, A. A. Hoffmann, M. Turelli, *PLoS ONE*. **6**, e22565 (2011).
11. R. Zug, P. Hammerstein, *Biol. Rev.* **90**, 89–111 (2015).
12. P. Kriesner, A. A. Hoffmann, S. F. Lee, M. Turelli, A. R. Weeks, *PLoS Pathog.* **9**, e1003607 (2013).
13. P. A. Ross *et al.*, *PLoS Negl. Trop. Dis.* **14**, e0007958 (2020).
14. A. A. Hoffmann, *Entomol. Exp. Appl.* **48**, 61–67 (1988).
15. A. A. Hoffmann, M. Hercus, H. Dagher, *Genetics*, 11 (1998).
16. K. T. Reynolds, A. A. Hoffmann, *Genet. Res.* **80** (2002), doi:10.1017/S0016672302005827.
17. E. M. Layton, J. On, J. I. Perlmutter, S. R. Bordenstein, J. D. Shropshire, *mBio*. **10**, e01879-19, /mbio/10/6/mBio.01879-19.atom (2019).
18. M. Solignac, D. Vautrin, F. Rousset, *Comptes Rendus Acad. Sci. - Ser. III*. **317**, 461–470 (1994).
19. R. L. Verspoor, P. R. Haddrill, *PLoS ONE*. **6**, e26318 (2011).
20. P. Kriesner, W. R. Conner, A. R. Weeks, M. Turelli, A. A. Hoffmann, *Evolution*. **70**, 979–997 (2016).
21. A. J. Fry, M. R. Palmer, D. M. Rand, *Heredity*. **93**, 379–389 (2004).
22. W. Harcombe, A. A. Hoffmann, *J. Invertebr. Pathol.* **87**, 45–50 (2004).

23. S. V. Serga, O. M. Maistrenko, N. P. Matiytsiv, A. M. Vaiserman, I. A. Kozeretska, *Symbiosis*. **83**, 163–172 (2021).
24. A. Strunov, S. Lerch, W. U. Blanckenhorn, W. J. Miller, M. Kapun, *J. Evol. Biol.* **35**, 788–802 (2022).
25. E. M. Fast *et al.*, *Science*. **334**, 990–992 (2011).
26. H. M. Frydman, J. M. Li, D. N. Robson, E. Wieschaus, *Nature*. **441**, 509–512 (2006).
27. V. Foray, M. M. Perez-Jimenez, N. Fattouh, F. Landmann, *Dev. Cell*. **45**, 198–211 (2018).
28. B. A. Pannebakker, B. Loppin, C. P. Elemans, L. Humblot, F. Vavre, *Proc. Natl. Acad. Sci.* **104**, 213–215 (2007).
29. S. L. Russell, J. R. Castillo, in *Symbiosis: Cellular, Molecular, Medical and Evolutionary Aspects*, M. Kloc, Ed. (Springer International Publishing, Cham, 2020; http://link.springer.com/10.1007/978-3-030-51849-3_5), vol. 69 of *Results and Problems in Cell Differentiation*, pp. 137–176.
30. D. J. Starr, T. W. Cline, *Nature*. **418**, 76 (2002).
31. H. A. Flores, J. E. Bubnell, C. F. Aquadro, D. A. Barbash, *PLoS Genet*. **11**, e1005453 (2015).
32. J. E. Bubnell, P. Fernandez-Begne, C. K. S. Ulbing, C. F. Aquadro, *G3 GenesGenomesGenetics* (2021), doi:10.1093/g3journal/jkab312.
33. M. Ote, M. Ueyama, D. Yamamoto, *Curr. Biol.* **26**, 2223–2232 (2016).
34. M. Ote, D. Yamamoto, *Arch. Insect Biochem. Physiol.* **99**, e21475 (2018).
35. Y. Li, N. T. Minor, J. K. Park, D. M. McKearin, J. Z. Maines, *Proc. Natl. Acad. Sci.* **106**, 9304–9309 (2009).
36. Y. Li, J. Z. Maines, O. Y. Tastan, D. M. McKearin, M. Buszczak, *Development*. **139**, 1547–1556 (2012).
37. R. A. Neumüller *et al.*, *Nature*. **454**, 241–245 (2008).
38. S. L. Page, K. S. McKim, B. Deneen, T. L. Van Hook, R. S. Hawley, *Genetics*. **155**, 1757 (2000).
39. J. J. Sekelsky *et al.*, *Genetics*. **152**, 529–542 (1999).
40. S. Aruna, H. A. Flores, D. A. Barbash, *Genetics*. **181**, 1437–1450 (2009).
41. M. Zaccai, H. D. Lipshitz, *Zygote*. **4**, 159–166 (1996).
42. M. E. Toomey, K. Panaram, E. M. Fast, C. Beatty, H. M. Frydman, *Proc. Natl. Acad. Sci.* **110**, 10788–10793 (2013).
43. T. D. Hinnant, J. A. Merkle, E. T. Ables, *Front. Cell Dev. Biol.* **8**, 19 (2020).
44. R. Zhao, Y. Xuan, X. Li, R. Xi, *Aging Cell*. **7**, 344–354 (2008).
45. T. T. Su, F. Sprenger, P. J. DiGregorio, S. D. Campbell, P. H. O'Farrell, *Genes Dev.* **12**, 1495–1503 (1998).
46. Y. Li *et al.*, *PLoS ONE*. **8**, e58301 (2013).
47. J. Chau, L. S. Kulnane, H. K. Salz, *Genetics*. **182**, 121–132 (2009).
48. C.-Y. Tseng *et al.*, *PLoS Genet.* **10**, e1004888 (2014).
49. J. Chau, L. S. Kulnane, H. K. Salz, *Proc. Natl. Acad. Sci.* **109**, 9465–9470 (2012).
50. Indrayani Waghmare, Andrea Page-McCaw, *Genes*. **9**, 127 (2018).
51. W. Joly, A. Chartier, P. Rojas-Rios, I. Busseau, M. Simonelig, *Stem Cell Rep.* **1**, 411–424 (2013).
52. S. Ji *et al.*, *Proc. Natl. Acad. Sci.* **114**, 6316–6321 (2017).
53. T. Xie, A. C. Spradling, *Science*. **290**, 328–330 (2000).
54. D. Chen, D. McKearin, *Curr. Biol.* **13**, 1786–1791 (2003).
55. X. Song *et al.*, *Development*. **131**, 1353–1364 (2004).
56. E. Glasscock, *Genetics*. **170**, 1677–1689 (2005).
57. H. Herranz *et al.*, *EMBO J.* **29**, 1688–1698 (2010).
58. A. Ferreira, L. Boulan, L. Perez, M. Milán, *Genetics*. **198**, 249–258 (2014).
59. C. S. Santoso *et al.*, *G3amp58 GenesGenomesGenetics*. **8**, 833–843 (2018).
60. V. Lantz, J. S. Chang, J. I. Horabin, D. Bopp, P. Schedl, *Genes Dev.* **8**, 598–613 (1994).
61. R. Kaur, B. A. Leigh, I. T. Ritchie, S. R. Bordenstein, *PLOS Biol.* **20**, e3001584 (2022).
62. M. Turelli, A. A. Hoffmann, *Genetics*. **140**, 1319 (1995).
63. E. Rastegari *et al.*, *Development*. **147**, dev182063 (2020).
64. C. Rhiner *et al.*, *Development*. **136**, 995–1006 (2009).
65. M. Ote, D. Yamamoto, *Curr. Opin. Insect Sci.* **37**, 8–15 (2020).
66. Z. Wang, H. Lin, *Dev. Biol.* **302**, 160–168 (2007).
67. Y. Ye, A. Godzik, *Genome Res.* **14**, 343–353 (2004).
68. N. W. Beebe *et al.*, *Proc. Natl. Acad. Sci.* **118**, e2106828118 (2021).